Journal of Photochemistry, 2 (1973/74) 139–149

NITRIC ACID VAPOUR ABSORPTION CROSS-SECTION SPECTRUM AND ITS PHOTODISSOCIATION IN THE STRATOSPHERE

F. BIAUME
Institut d'aeronomie spatiale de Belgique, 3, Avenue Circulaire, 1180 Brussels (Belgium)
(Received March 29, 1973; in revised form April 9, 1973)

SUMMARY

Absorption cross-section values of nitric acid vapour at room temperature have been measured at different wavelengths in the 1850–3250 Å spectral range. In conjuction with recently published data, they lead to a precise HNO_3 absorption curve. Estimates, assuming a quantum yield equal to unity, are also given for the nitric acid photodissociation coefficient in the stratosphere.

INTRODUCTION

Nitric acid, which has recently been observed in the stratosphere by Murcray *et al.*[1,2] is related to the nitrogen oxides[3]. An accurate determination of its stratospheric distribution is thus necessary to estimate the behaviour of minor constituents such as nitrogen dioxide and hydroxyl radical[4]. Nitric acid is produced by the reaction:

$$(b_{22});\ NO_2 + OH + M \rightarrow HNO_3 + M \qquad (1)$$

and is destroyed by the two-body reaction:

$$(b_{27});\ HNO_3 + OH \rightarrow NO_3 + H_2O \qquad (2)$$

or in a sunlit atmosphere, by photodissociation processes[5,6]:

$$(J_{HNO_3});\ HNO_3 + h\nu\ (\lambda < 5980\ \text{Å}) \rightarrow NO_2 + OH \qquad (3a)$$

$$HNO_3 + h\nu\ (\lambda < 4010\ \text{Å}) \rightarrow HNO_2 + O(^3P) \qquad (3b)$$

$$HNO_3 + h\nu\ (\lambda < 2900\ \text{Å}) \rightarrow NO_3 + H \qquad (3c)$$

$$HNO_3 + h\nu\ (\lambda < 2450\ \text{Å}) \rightarrow HNO_2 + O(^1D) \qquad (3d)$$

The nitric acid concentration is thus very sensitive to the OH profile and to the vertical distribution of the photodissociation mechanisms. Therefore, precise measurements of the HNO_3 absorption cross-section are required in the u. v. spectral range where the photodissociation takes place.

Since the pioneer work of Dalmon[7] only two measurements of the nitric acid u. v. absorption spectrum by Schmidt *et al.*[8] and by Johnston and Graham[6], have been made. This paper reports measurements at the wavelengths of 37 atomic lines in the 1850–3650 Å spectral range. Using these new data, the nitric acid photodissociation coefficient is presented for different wavelength intervals and various altitudes. The results show two large spectral contributions which are situated in the 2000 Å atmospheric window and at $\lambda > 3000$ Å. According to reactions (3a), (3b), (3c) and (3d), they may represent different dissociation processes.

EXPERIMENTAL

The instrumentation used in this study has already been described in detail[9,10]. Briefly, it consisted of a 50 cm focal length Bausch and Lomb grating monochromator in conjunction with a 400.5 cm length absorption cell and an EMI 6255 Mg photomultiplier. The absorption cell, sealed at each end with a Suprasil quartz lens, was connected to a gas handling system provided with reservoirs, traps and manometers. The whole system, which could be evacuated down to 10^{-6} Torr, was constructed in Pyrex and equipped with silicone greased stopcocks.

The nitric acid was prepared by molecular distillation at low temperature and in the dark in order to prevent thermal and photodecomposition. High purity HNO_3 was distilled under vacuum (10^{-5} Torr) from a bulb containing a sulphonitric mixture (40% HNO_3 at min. 65% and 60% H_2SO_4 at min. 96%; Merck, Darmstadt, FGR) maintained at 0°C into a trap cooled at liquid nitrogen temperature. This procedure was followed by several successive distillations from trap to trap at 0°C and −196°C respectively in order to remove evacuable impurities like N_2 and O_2. The product was finally stored as a white crystalline solid at liquid nitrogen temperature in a reservoir closed by a greaseless Teflon O-ring stopcock.

Since nitric acid has a continuous absorption, the measurements were made at the different line wavelengths emitted by a $SiCl_4$ microwave lamp[11] and by Hg, Cd, Zn and Hg discharge lamps manufactured by Philips. The lines of proper wavelength were selected in the first order of the monochromator and their light intensity was measured by the photomultiplier after passage through the absorption cell which was either evacuated or filled with the nitric acid vapour at various pressures.

For each absorption measurement in the 2000–3000 Å region nitric acid was warmed up to 0°C and the gas phase was introduced into the absorption cell at pressures varying from $\simeq$ 0 to 14 Torr. At wavelengths larger than 3000 Å, the reservoir containing the acid was warmed up to the room temperature in order to obtain a measurable absorption by the use of pressures, up to 45 Torr. On the

contrary, very low pressures were needed at wavelengths below 2000 Å, as the absorption of nitric acid increases importantly. In these conditions, different gas samples were collected in a small section of the gas handling system and then expanded into the absorption cell. The volume ratio [$v/v + V = 2.096 \times 10^{-2}$] between the gas handling system and the cell was established experimentally by two absorption measurements at 2124.1 Å realised by direct introduction and by expansion of the gas respectively. Pressure measurements in excess of 14 Torr were made by means of a Bourdon gauge balanced by air pressure read on a mercury manometer; a silicone oil manometer read with a cathetometer was used for lower values.

RESULTS AND DISCUSSION

The absorption cross-section values obtained at various wavelengths were deduced from the experimental data according to the Beer's law expression:

$$\sigma_\lambda = \left[n_0 \frac{P}{P_0} \frac{T_0}{T} d \right]^{-1} \times 2.303 \log_{10} \frac{I_0}{I} \tag{4}$$

where σ_λ (cm^2) is the absorption cross-section; n_0 (2.6872×10^{19} part. cm^{-3}) is Loschmidt number; P_0 (760 Torr) and T_0 (273.16 K) are respectively the pressure and temperature in standard conditions; d (400.5 cm) is the pathlength used and $\log_{10} I_0/I$ corresponds to the observed optical density.

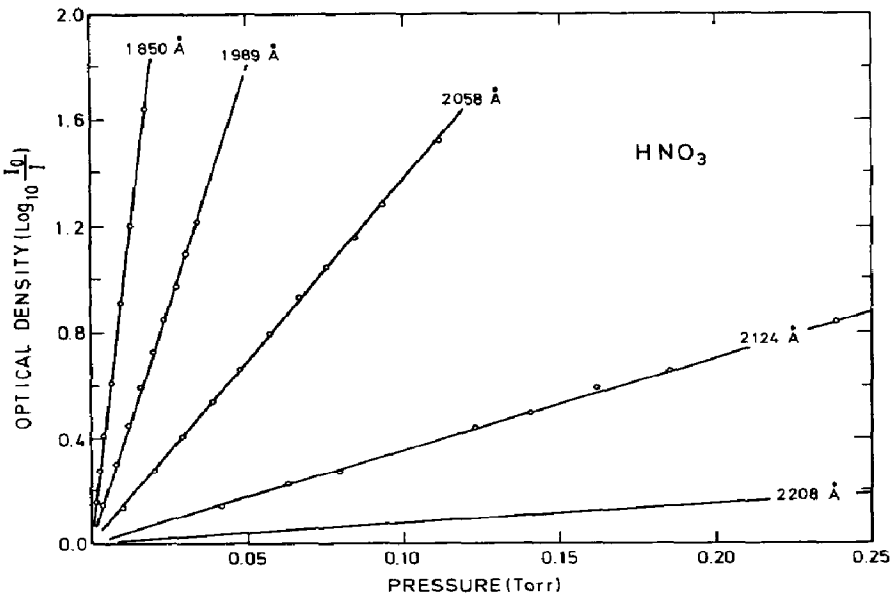

Fig. 1. Nitric acid optical density *vs.* pressure for various wavelengths in the 1850–2200 Å spectral range.

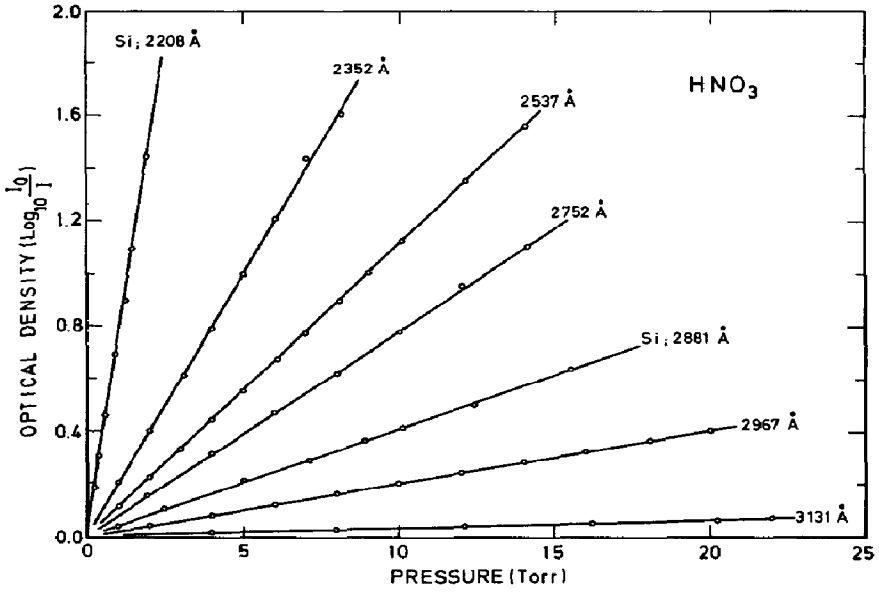

Fig. 2. Nitric acid optical density *vs.* pressure for various wavelengths in the 2200–3100 Å spectral range.

This linear relation (4) can be applied (see Figs. 1 and 2) to the measurements which did not require nitric acid vapour pressure exceeding 20 Torr in the 400.5 cm absorption cell which is used here. It is also the case for every measurement performed at shorter wavelengths than 3200 Å where the absorption cross-section is not too small.

A systematic departure from Beer's law was observed for the other measurements; this is shown in Fig. 3 and characterized by a non-linear increase of the optical density above a certain pressure ($\simeq$ 25 Torr). This departure could be due either to condensation on the windows of the absorption cell—as the acid contained in the storage reservoir must be warmed to get rapidly needed pressure—or to nitrogen oxides formed by thermal decomposition or by reaction of HNO_3 with the silicone grease of the stopcocks. In these particular cases, the absorption cross-section values were determined from the linear portions of the optical density curves presented in Fig. 3.

In order to detect traces of nitrogen dioxide in the nitric acid, absorption measurements were made in the 3300–3650 Å spectral range assuming that nitric acid does not practically absorb at those wavelengths[6]. A concentration ratio $[NO_2]/[HNO_3]$ of about $(4.5 \pm 0.5) \times 10^{-4}$ was found comparing the experimental results (see Fig. 4) with the NO_2 absorption curve of Hall and Blacet[12]. From 3000 to 3250 Å, the absorption contribution due to NO_2, deduced from this curve, was taken into account in the experimental results. No correction for nitrogen tetroxide absorption was made, since in the present experiments, the maximum

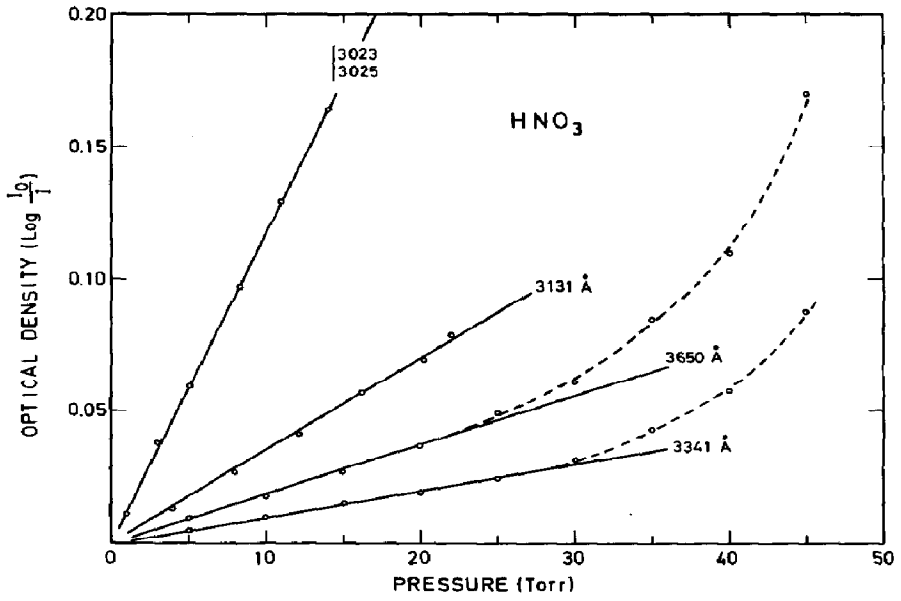

Fig. 3. Nitric acid optical density *vs.* pressure for various wavelengths in the 3000–3650 Å spectral range. The departure from Beer's law appears above 20 Torr, for the measurements at 3341 and 3650 Å.

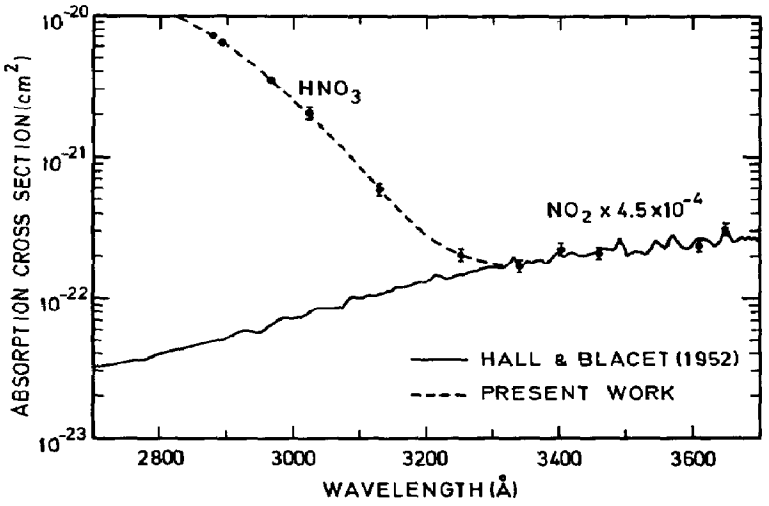

Fig. 4. Absorption cross-section measurements in the 2700–3700 Å spectral range. The contribution due to nitrogen dioxide above 3250 Å is shown by Hall and Blacet's NO_2 absorption curve which is multiplied by 4.5×10^{-4} in order to fit our experimental results.

value of the $[N_2O_4]/[NO_2]$ relative concentration estimated from the $N_2O_4 \rightleftharpoons 2\ NO_2$ equilibrium constant of Verhoek and Daniels[13], would be of the order of 3×10^{-4}.

The absorption cross-section values are given in Table 1. Probable experimental errors are estimated to $\pm$ 3% in the 1850–2100 Å region, $\pm$ 1% in the 2100–3000 Å region and about $\pm$ 10% above 3000 Å. Figure 5 represents the best fit curve throughout the experimental points and shows the NO_2 absorption contribution above 3000 Å. Excellent agreement appears in this Figure with the recent measurements of Johnston and Graham[6]. Only slight differences exist at both ends of the absorption curve where the experimental errors are the largest. However, the value of 2×10^{-23} cm^2 adopted by these authors at 3250 Å seems to be somewhat low and could be due to an overestimation of the NO_2 quantity present in their HNO_3. Nevertheless, as it will be shown below, this discrepancy could not play an important role in aeronomic applications.

TABLE 1

ABSORPTION CROSS-SECTIONS OF NITRIC ACID VAPOUR

Line wavelength (Å)	Element	Cross-section (cm^2)	Line wavelength (Å)	Element	Cross-section (cm^2)
1849.9	Hg	1.63×10^{-17}	2698.9	Hg	1.64×10^{-20}
1942.3	Hg	1.16	2699.5	Hg	
1988.9	Si	6.19×10^{-18}	2752.2	Hg	1.36
2058.1	Si	2.39	2758.8	Hg	
2124.1	Si	6.12×10^{-19}	2803.5	Hg	1.09
2207.9	Si	1.32	2804.5	Hg	
2216.6	Si	1.20	2881.6	Si	7.15×10^{-21}
2218.0	Si		2893.6	Hg	6.42
2302.1	Hg	5.35×10^{-20}	2967.3	Hg	3.57
2352.5	Hg	3.49	2967.6	Hg	
2378.3	Hg	2.97	3023.5	Hg	2.06*
2399.4	Hg	2.61	3025.6	Hg	
2399.7	Hg		3131.5	Hg	6.02×10^{-22}*
2435.1	Si	2.15	3131.8	Hg	
2484.8	Hg	1.98	3252.5	Cd	2.09*
2506.9	Si	1.94	3341.5	Hg	1.71
2514.3	Si	1.94	3403.6	Cd	2.33
2516.1	Si		3466.2	Cd	2.13
2519.2	Si	1.94	3612.9	Cd	2.44
2524.1	Si	1.94	3650.1	Hg	3.20
2528.5	Si	1.94			
2532.3	Si	1.94	3023.5	Hg	1.98×10^{-22}
2536.5	Hg	1.95	3025.6	Hg	
2576.3	Hg	1.93	3131.5	Hg	4.9
2631.2	Si	1.81	3131.8	Hg	
2652.0	Hg	1.77	3252.5	Cd	6.0×10^{-23}

* These values include the NO_2 absorption contribution. The corrected values are listed at the end of the Table.

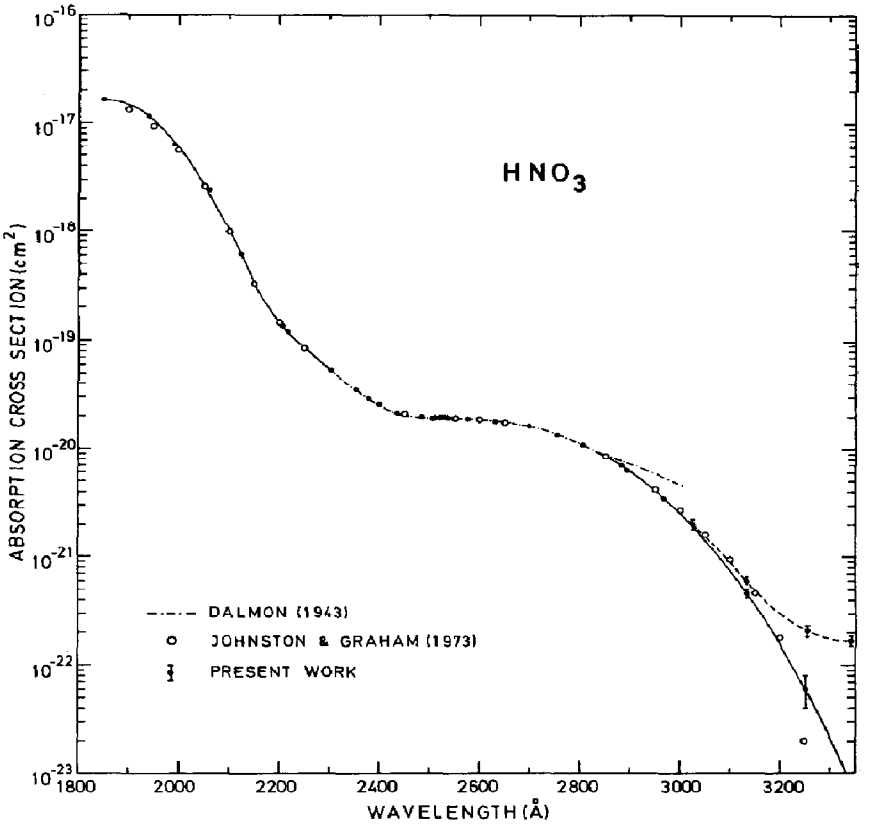

Fig. 5. Nitric acid absorption cross-section measurements in the 1850–3350 Å spectral range. The very good agreement between the present results and the recent data of Johnston and Graham leads to an accurate HNO_3 u.v. absorption curve.

NITRIC ACID STRATOSPHERIC PHOTODISSOCIATION

In order to estimate the aeronomic implications of the HNO_3 absorption in the u.v. spectral range, the averaged absorption cross-section values listed in Table 2 have been adopted to each wavenumber interval of the solar flux used by Ackerman[14]. Assuming* a quantum yield equal to unity[15] the nitric acid photodissociation coefficient J_{HNO_3} has then been computed according to the formula:

$$J_{HNO_3} = \sum_{\Delta\nu_i} \sigma_{HNO_3}(\Delta\nu_i) \times \Phi_z(\Delta\nu_i) \qquad (5)$$

where $\sigma_{HNO_3}(\Delta\nu_i)$, ($cm^2$) and $\Phi_z(\Delta\nu_i)$, (cm^{-2}, s^{-1}) are respectively the HNO_3 absorption cross-section and the solar flux at altitude z, averaged in the same wavenumber interval $\Delta\nu_i$.

* The author regards this estimate of the quantum yield by Johnston[15] to be more reliable than the lower figures quoted by other workers.

TABLE 2

AVERAGED ABSORPTION CROSS-SECTION VALUES FOR NITRIC ACID VAPOUR

Wavenumber interval (cm^{-1})	Wavelength interval (Å)	Averaged cross-section (cm^2)	Wavenumber interval (cm^{-1})	Wavelength interval (Å)	Averaged cross-section (cm^2)
54,000–53,500	1852–1869	1.62×10^{-17}	41,000–40,500	2439–2469	2.05×10^{-20}
53,500–53,000	1869–1887	1.58	40,500–40,000	2469–2500	1.97
53,000–52,500	1887–1905	1.47	40,000–39,500	2500–2532	1.94
52,500–52,000	1905–1923	1.37	39,500–39,000	2532–2564	1.94
52,000–51,500	1923–1942	1.21	39,000–38,500	2564–2597	1.92
51,500–51,000	1942–1961	1.01	38,500–38,000	2597–2632	1.86
51,000–50,500	1961–1980	8.00×10^{-18}	38,000–37,500	2632–2667	1.78
50,500–50,000	1980–2000	6.50	37,500–37,000	2667–2703	1.67
50,000–49,500	2000–2020	4.81	37,000–36,500	2703–2740	1.52
49,500–49,000	2020–2041	3.56	36,500–36,000	2740–2778	1.34
49,000–48,500	2041–2062	2.46	36,000–35,500	2778–2817	1.14
48,500–48,000	2062–2083	1.71	35,500–35,000	2817–2857	9.29×10^{-21}
48,000–47,500	2083–2105	1.12	35,000–34,500	2857–2899	7.15
47,500–47,000	2105–2128	7.56×10^{-19}	34,500–34,000	2899–2941	5.33
47,000–46,500	2128–2150	4.66	34,000–33,500	2941–2985	3.65
46,500–46,000	2150–2174	3.21	33,500–33,000	2985–3030	2.41
46,000–45,500	2174–2198	2.07	33,000–32,500	3030–3077	1.45
45,500–45,000	2198–2222	1.35	32,500–32,000	3100 ± 25	7.86×10^{-22}
45,000–44,500	2222–2247	9.70×10^{-20}	32,000–31,496	3150	3.75
44,500–44,000	2247–2273	7.53	31,496–31,008	3200	1.62
44,000–43,500	2273–2299	6.00	31,008–30,534	3250	6.50×10^{-23}
43,500–43,000	2299–2326	4.98	30,534–30,075	3300	2.60*
43,000–42,500	2326–2353	4.03	30,075–29,630	3350	1.03*
42,500–42,000	2353–2381	3.25	29,630–29,197	3400	4.10×10^{-24}*
42,000–41,500	2381–2410	2.64	29,197–28,777	3450	1.60*
41,500–41,000	2410–2439	2.29			

* Extrapolated values.

At the top of the atmosphere (see Fig. 6), the photodissociation reaches a maximum near 2000 Å and falls off by more than an order of magnitude towards 2500 Å where the decrease of the HNO_3 absorption cross-section is counterbalanced by the increase of the solar flux. At wavelengths larger than 3000 Å, the contribution to J_{HNO_3} becomes negligible since the absorption cross-section decreases very sharply. An integration over the whole 1850–3450 Å spectral range leads to a total photodissociation coefficient of 1.7×10^{-4} s^{-1} at the top of the atmosphere. This value represents a lower limit as the contribution below 1850 Å still seems to be large[8]. Nevertheless, this contribution can be neglected in the whole stratosphere since the u.v. solar radiation shorter than 1850 Å is absorbed in the mesosphere by the Schumann–Runge system of molecular oxygen[16,17].

The ozone absorption strongly reduces the dissociation rate in the 2200–2900 Å region. For example, at 2500 Å where the O_3 absorption reaches a maximum, J_{HNO_3} decreases by about two orders of magnitude at 40 km if the atmospheric

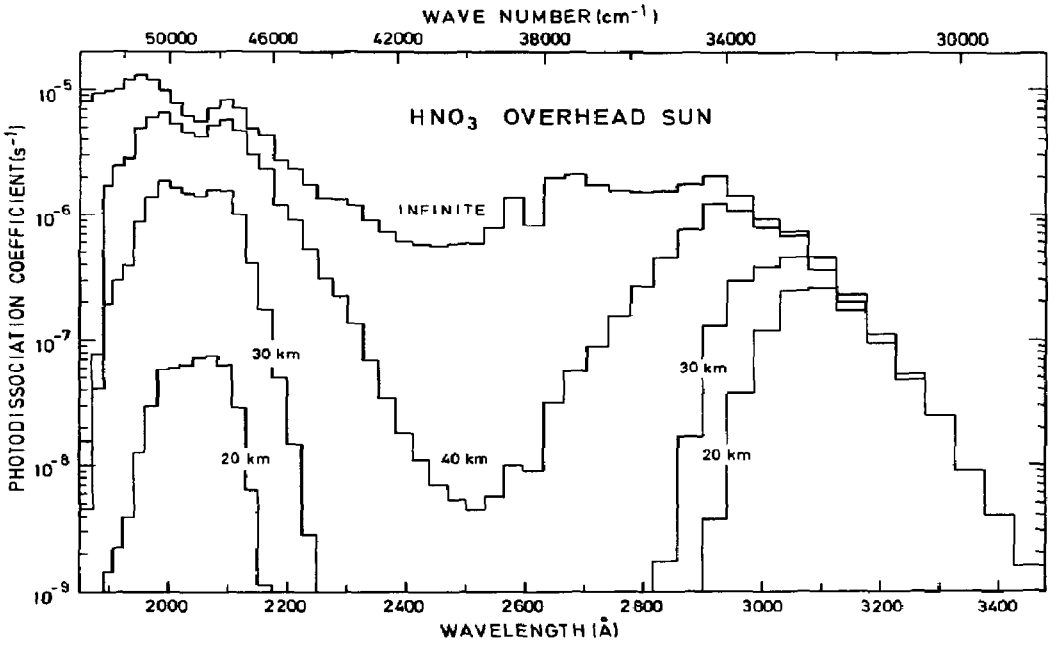

Fig. 6. Nitric acid photodissociation coefficient *vs.* wavelength for overhead Sun conditions and various altitudes. The decrease of J_{HNO_3} in the 2200–2900 Å spectral range and below 2000 Å is due to the absorption of the solar flux by stratospheric ozone and by molecular oxygen respectively.

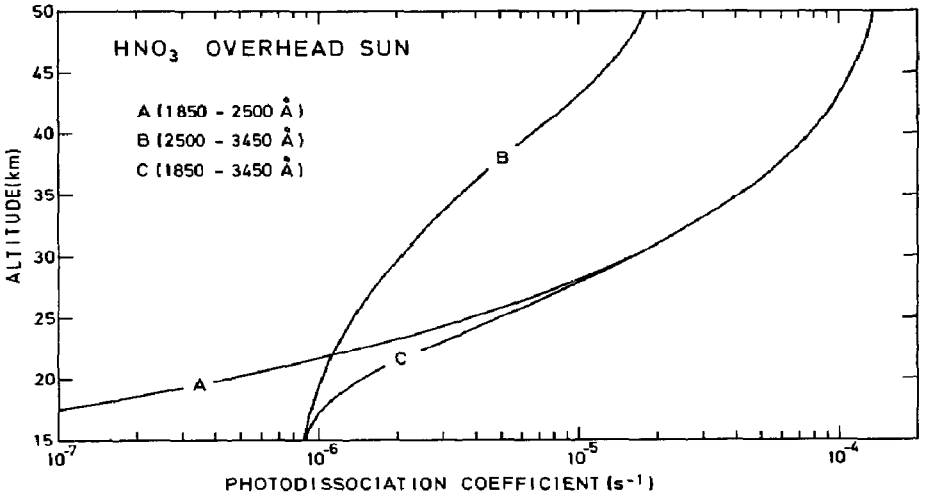

Fig. 7. Photodissociation coefficient of nitric acid in the stratosphere for two complementary spectral ranges and overhead sun conditions. As shown by curves A, B and C, HNO_3 is mostly dissociated by the short wavelength range of the solar flux in the upper stratosphere and by the long wavelength range in the lower stratosphere.

model deduced by Nicolet[18,19] is adopted for overhead sun conditions. Then, in the stratosphere, two spectral intervals play a major role. The first one, around 2000 Å, is the most important at high altitudes and the second one, at about 3000 Å, becomes dominant in the lower stratosphere, since the absorption of the solar radiation is very weak in this spectral range. In order to illustrate this double effect, the stratospheric J_{HNO_3}, calculated for two partial spectral ranges (1850–2500 Å and 2500–3450 Å), is represented in Fig. 7 as well as the total value. This Figure shows clearly that nitric acid photodissociation above 30 km, is mostly due to the absorption in the 1850–2500 Å region since the values from curve A are larger than those from curve B by about a factor of 10. This situation is inverted in the lower stratosphere and in the troposphere where the influence of the 2500–3450 Å radiation becomes dominant.

Finally, the total photodissociation coefficient, calculated for different solar zenith anglse, is plotted *versus* altitude in Fig. 8. Its value, depending on different solar conditions is about 10^{-4} s^{-1} at the stratopause and slowly decreases to reach 10^{-6} to 10^{-7} s^{-1} at the tropopause.

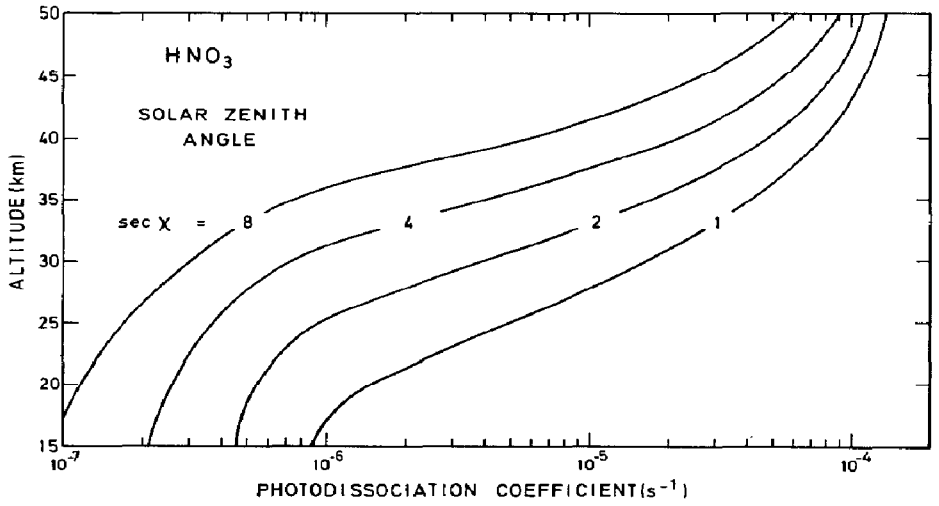

Fig. 8. Photodissociation coefficient of nitric acid in the stratosphere for various solar zenith angles. From overhead sun conditions, $\chi = 0°$ to $\chi = 83°$.

CONCLUSIONS

The present absorption cross-section measurements are in excellent agreement with the recent data published by Johnston and Graham[6]. They lead to a precise absorption curve from 1850 to 3250 Å and confirm the early measurements of Dalmon[7], over a shorter wavelength interval. The HNO_3 absorption related by Schmidt *et al.*[8] could not be detected above 3300 Å, where the contribution of NO_2 cannot be neglected.

The estimate of the nitric acid photodissociation coefficient shows that this loss process is important, but more information concerning the dissociation mechanisms involved in the investigated spectral range is still needed in order to explain the aeronomic behaviour of HNO_3 in the lower stratosphere.

ACKNOWLEDGEMENTS

The author is deeply grateful to Professor M. Nicolet for his particular interest and valuable advice during the preparation of this work. He also wishes to express his thanks to Mr. G. Brasseur for his useful help and discussions.

REFERENCES

1 D. G. Murcray, T. G. Kyle, F. H. Murcray and W. J. Williams, *Nature*, 78 (1968) 218.
2 D. G. Murcray, T. G. Kyle, F. H. Murcray and W. J. Williams, *J. Opt. Soc. Am.*, 59 (1969) 1131.
3 M. Nicolet, *J. Geophys. Res.*, 70 (1965) 679.
4 G. Brasseur and M. Nicolet, *Aeronomica Acta*, A (1973) 113; *Plant. Space Sci.*, (1973) in press.
5 H. Okabe, Chemical kinetics data survey II, *NBS Rep.* (1972) 10828.
6 H. S. Johnston and R. Graham, *J. Phys. Chem.*, 77 (1973) 62.
7 R. Dalmon, *Mém. Serv. Chim. Etat*, 30 (1943) 141.
8 S. C. Schmidt, R. C. Amme, D. G. Murcray, A. Goldman and F. S. Bonomo, *Nature (Phys. Sci.)*, 238 (1972) 109.
9 M. Ackerman, F. Biaume and G. Kockarts, *Plan Space Sci.*, 18 (1970) 1639.
10 F. Biaume, Thèse de Doctorat ULB Mars, 1972, *Aeronomica Acta*, A (1972) 100.
11 V. Kaufman, L. J. Radziemski Jr. and K. L. Andrew, *J. Opt. Soc. Am.*, 56 (1966) 911.
12 T. C. Hall and F. E. Blacet, *J. Chem. Phys.*, 20 (1952) 1745.
13 F. H. Verhoek and F. Daniels, *J. Am. Chem. Soc.*, 53 (1931) 1250.
14 M. Ackerman, *Aeronomica Acta*, A (1970) 77; in G. Fiocco, (ed.), *Mesospheric Models and Related Experiments*, Reidel, Dordrecht, Holland, 1971, p. 149.
15 H. S. Johnston, *CIAP 72-4 Newsletter*, Dec. 8, (1972).
16 G. Kockarts, *Aeronomica Acta*, A (1970) 78; in Fiocco, G. (ed.), *Mesospheric Models and Related Experiments*, Reidel, Dordrecht, Holland, 1971, p. 160.
17 G. Kockarts, *Aeronomica Acta*, A (1972) 107.
18 M. Nicolet, *Ann. Geophys.*, 26 (1970) 531.
19 M. Nicolet, *Aeronomica Acta*, A (1970) 79; in Fiocco, G. (ed.), *Mesospheric Models and Related Experiments*, Reidel, Dordrecht, Holland, 1971, p. 1.